Hindawi
International Journal of Optics
Volume 2020, Article ID 3160837, 7 pages
https://doi.org/10.1155/2020/3160837

Research Article

High-Visibility Pseudothermal Light Source Based on a Cr^{4+} : YAG Passively Q-Switched Single-Longitudinal-Mode Laser

Can Cui,[1] **Yulei Wang**,[2] **Zhiwei Lu**,[1,2] **Zhenxu Bai**,[2,3] **Hang Yuan**,[1] **Yi Chen**,[4] **and Yue Wang**[1]

[1]*National Key Laboratory of Science and Technology on Tunable Laser, Harbin Institute of Technology, Harbin 150080, China*
[2]*Hebei Key Laboratory of Advanced Laser Technology and Equipment, Center for Advanced Laser Technology, Hebei University of Technology, Tianjin 300401, China*
[3]*Photonics Research Centre, Department of Physics and Astronomy, Macquarie University, Sydney, NSW 2109, Australia*
[4]*China Jiliang University, College of Optical and Electronics and Information Engineering, Tianjin 300401, China*

Correspondence should be addressed to Yulei Wang; wyl@hebut.edu.cn and Zhiwei Lu; zw_lu@sohu.com

Received 24 July 2020; Revised 21 September 2020; Accepted 14 October 2020; Published 5 November 2020

Academic Editor: Chenggen Quan

High-visibility pseudothermal light source is required by the long-distance ghost imaging technology. In this article, the pulsed pseudothermal light based on a compact and Q-switched laser system with high peak power and intensity is reported. The passively Q-switched technique advances the performance of the pseudothermal light, where the second-order quantum correlation function $g^{(2)}$ value increased from 1.452 to 1.963.

1. Introduction

Ghost image (GI) is the acquisition of object information by means of photocurrent correlation measurements. Due to its unique physical characteristics, ghost imaging has been widely applied into many fields, such as high-resolution object reconstruction, remote sensing LiDAR, and optical security. With the development of GI, pseudothermal light is increasingly preferred as a choice of the light source during the last two decades [1–3]. GI was originally performed with entangle-photon pairs produced by spontaneous parametrical down-conversion and subsequently realized by using pseudothermal sources [4–6]. The pseudothermal light source, also known as quasi-thermal source, is a narrow band thermal light, which can be simulated by a rotating diffusing disk illuminated by coherent light, such as a laser beam. With the different rotation speed of the ground glass plate, the coherence time of the pseudothermal light can be optimized from 10 to 5 to 1 sec. Compared to the entangle-photon pair scheme, the imaging intensity of pseudothermal GI goes higher, which facilitates the technique applicable for more occasions. Unlike the real-thermal light, pseudothermal light has longer coherence time, which improves the accuracy of the instantaneous fluctuation intensity measurement and obtains higher signal-to-noise ratio (SNR) images as a result.

Continuous pseudothermal light has been proved it does not satisfy the cross spectrum condition of the classic thermal light, which causes the inadequate detection of the light field thermal fluctuations under the limitation of the photodetector response time [7–9]. Pulsed pseudothermal light, however, obeys the Gaussian distribution like the classic thermal light, and this optical field also obeys the cross spectrum purity condition, whose fluctuation can be accurately detected by the slow response detector. With the characteristic of high energy, short duration, and single-longitudinal mode, this high quality ideal imaging light source makes it possible to expand the applications of GI into LiDAR, space exploration, remote imaging, etc. [4] and again attracts people attention recently. The development of the airborne three-dimensional ghost imaging LiDAR imaging motional targets require high energy, high visibility

and brightness, and high-stability pseudothermal light source to avoid the attenuation during the propagation, the influence from the background radiation, and the unstable air environment [10–13]. Therefore, nanosecond laser pulse with high energy becomes an ideal choice.

The active and the passive Q-switched techniques are generally adopted to obtain the nanosecond laser pulses. In an active Q-switched laser system, a longitudinal mode selection device has to be equipped to guarantee the laser output coherence, which makes the structure of the laser cavity more complicated. Passively Q-switched laser generates the nanosecond pulses by using the saturation absorbers of different initial transmission to achieve different time-duration pulses. With two parallel sides and the nonlinear saturation characteristics, the crystal also acts as a cavity longitudinal mode selector, which simplifies the structure and increase the optical stability of the oscillator [14, 15]. In our work, the passive Q-switched method has been chosen to obtain the high-brightness and high-power nanosecond laser pulse.

In this paper, we improve the performance of the pseudothermal light source by using a compact laser structure based on the passive Q-switched techniques and frequency doubling with KTP crystal, where the pulse energy exceeding 500 mJ and the high coherence are suitable for the ghost imaging. In Section 1, we first introduced the character of ghost imaging and the principles of selecting a light source fit for ghost imaging. In Section 2, we give the quantified relations to evaluate the performance of the light source. In Section 3 and Section 4, we introduce the compact structure and discuss the results of the experiment. In Section 5, we make a conclusion and expectation of this light source for GI.

2. Materials and Methods

The relation between laser coherence and second-order quantum correlation function of pseudothermal light field is studied.

The statistical characteristics of the random fluctuation of the light field are usually measured by the normalized second-order correlation function. Given the space-time point $(r_1,\ t_1)$ and $(r_2,\ t\ )$, the normalized second-order correlation function is defined as follows [13, 14, 16–18]:

$$g^{(2)}(r_1,t_1,r_2,t_2)=\frac{\langle I_1(r_1,t_1)I_2(r_2,t_2)\rangle}{\langle I_1(r_1,t_1)\rangle\langle I_2(r_2,t_2)\rangle}. \tag{1}$$

The physical significance of the formula above does not only represent the thermal fluctuation of the light field in terms of space and time but reveals the SNR of the spot images recorded by the scientific CCD. More explicitly, the formula can be derived into

$$\begin{aligned} g^{(2)}(r_1=r_2,t_1=t_2)&=\frac{\langle I_1(r_1,t_1)I_2(r_2,t_2)\rangle}{\langle I_1(r_1,t_1)\rangle\langle I_2(r_2,t_2)\rangle}\\ &=1+\frac{\langle\Delta I\rangle^2}{I^2}. \end{aligned} \tag{2}$$

The square of the inverse of SNR is involved. For the classic thermal light field, $g^{(2)}$ is equal to 2. Therefore, the pseudothermal light field has to infinitely converge to 2, to simulate the thermal fluctuations, in order to achieve high-quality GI images.

Considering the influence of laser bandwidth on the pseudothermal light, we assume that there are two single-longitudinal laser beams diffracted by the ground glass, which are independent on the frequency γ and the phase φ. l_1 and l_2 are the optical path of two laser beams. The intensity correlation can be written as [19]

$$\begin{aligned} \langle I_{iQ}I_{jQ}^{*}\rangle &= I_1^2\exp\left[i\left(\varphi_i-\varphi_j\right)+\gamma_1\frac{l_1-l_2}{c}\right]\\ &\quad+I_2^2\exp\left[i\left(\varphi_i-\varphi_j\right)+\gamma_2\frac{l_1-l_2}{c}\right], \end{aligned} \tag{3}$$

when the frequency difference satisfies,

$$\Delta\gamma=\gamma_1-\gamma_2<\frac{c}{4\left(l_1-l_2\right)}, \tag{4}$$

we consider the spot on the image which produces within bandwidth is identical, and the contrast of the spot is improved and the pseudothermal light of high quality is going to be achieved. As a result, the single-longitudinal mode and narrow bandwidth are the important parameters of a laser source which is needed for a better performance of the pseudothermal light output.

2.1. Experiment Setup. The schematic of the designed experimental setup is shown in Figure 1. The system consists of five parts, a passive Q-switched single longitudinal oscillator, a beam expander, the double-pass amplifier I, the single-pass amplifier II and the frequency doubling, and the measurement system. The optical isolator is set on the appropriate position to protect the front device from the leaking laser. Considering the independence of the isolator function and the aesthetics of illustration, the optical isolator is omitted from the picture.

Part 1 is the single longitudinal oscillator. A Nd : YAG rod ($\Phi 3\,\text{mm}\times 125\,\text{mm}$) doped with 1.0 at.% concentration of Nd^{3+} and antireflection (AR) coated at 1064 nm on both end faces was applied as gain medium. The Cr^{4+} : YAG crystal was used as passively Q-switched device for its relatively low thermal expansion coefficient ($7.7\times10^{-6}/^{\circ}\text{C}$) with initial transmission of 7.96% and was also used as a longitudinal mode selector for its nonlinear saturation characteristics. The resonator cavity was compact plane-plane configuration. $M1$ is a high reflectivity (HR) mirror at 1064 nm. $M2$ is a flat mirror with reflectivity of 60% at 1064 nm as an output coupler (OC). P is a Brewster angle polarizer. AD is an aperture diaphragm to filter the high-order transverse mode. The laser cavity operates just at the threshold of 22 J pump energy to lower the beam divergence angle and narrow the bandwidth of the laser output.

Part 2 is the beam expander with a factor of 3 ($L1$ is a plane-concave lens with $R=-50$ mm, and $L2$ is a

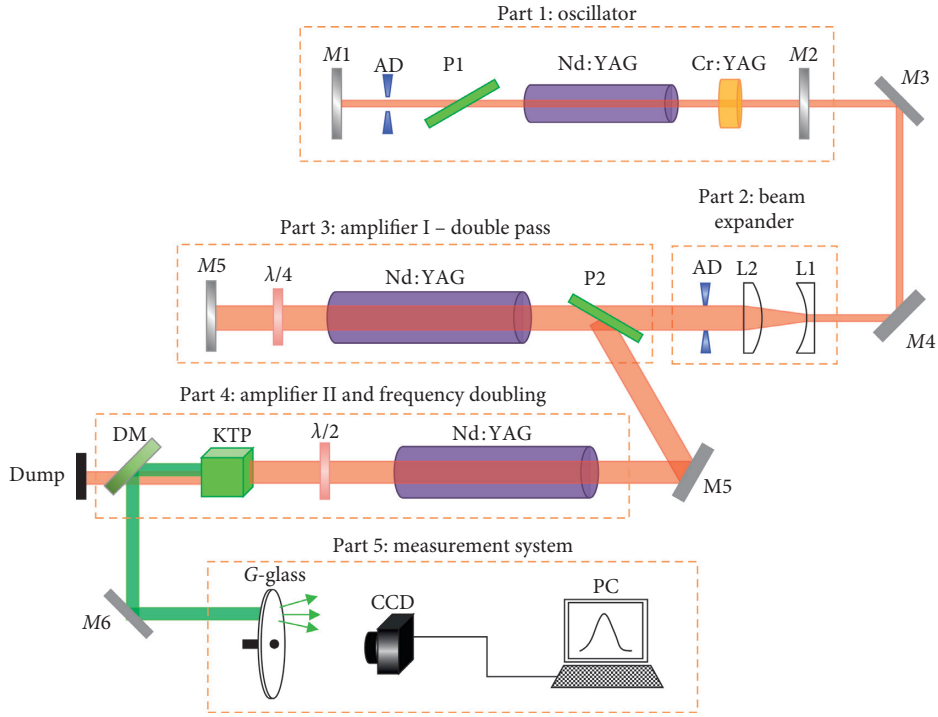

Figure 1: Schematic of the high-visibility pseudothermal ghost imaging laser experiment setup.

planoconvex lens with $R = 150$ mm). It is used to expand the diameter of the laser beam from the oscillator to improve the energy extraction efficiency of the amplifier and optimize the beam quality.

Part 3 is a double-pass amplifier with a $\Phi 8$ mm $\times$ 145 mm Nd : YAG rod. The doping concentration of the Nd : YAG crystal in two amplification stages is 1.0 at%. The configuration compensates the insufficient amplification resulting from the seed laser of low fluence.

Part 4 is a single-pass amplifier and the frequency doubler. The amplifier has the same specifications as the double-pass one. A $10 \times 10 \times 10$ mm^3 KTP crystal cut at type-II phase matching angle with $\theta = 90^\circ$, $\varphi = 24.59^\circ$was adopted as the frequency doubling device, which is fitted on a heat sink. Both surfaces of the crystal were AR-coated at 1064 nm and 532 nm. KTP is the most widely used commercial SHG material. The damage threshold of KTP is over 500 MW/cm^2, and compared to other nonlinear crystals as BBO, LBO, etc., KTP has very high frequency doubling efficiency, which makes it the best candidate for nanosecond laser frequency conversion. Half plate was used to adjust the laser beam phase matched with the frequency conversion crystal. DM is a dichroic mirror used to separate the infra-red and green laser, which is AR-coated at 1064 nm and HR-coated at 532 nm.

Parts 1–4 are composed of the laser system, where the laser crystals are pumped by the flashlamps, and the circulation of the cooling water of 20°C carries away the waste heat, which assures the safe and stable operation under 1–10 Hz work repetition.

Part 5 is a second-order correlation function measurement system setup. The frequency-doubling laser diffracted by the rotating ground glass under the appropriate speed was measured by the scientific CCD controlled by a computer, and the spot images recorded are transferred to the computer for the calculation. To prevent the camera from the overloading damage, the attenuator has to be set in front of the CCD.

We use the Fabry-Perot interferometer SA210-8B and SA201-EC manufactured by Thorlabs Inc., to measure the linewidth of the passively Q-switched pulses. Scanning F–P interferometer technique is the basic method for measuring many kinds of spectroscopies. Figure 2 shows schematically the layout for the laser linewidth measurement using this method. We use the oscilloscope and the computer program to get the integrated spectrum. From the spectrum, the laser linewidth can be determined by the free spectral range (FSR) of the FPI. The FPI we use in our experiment has the FSR of 10 GHz and the resolution of 67 MHz, and the photodiode has high sensitivity.

3. Results and Discussion

The laser system provides 6.8 ns pulses of 1064 nm and 5 ns pulses of 532 nm, with the waveforms illustrated in the Figure 3(a). The actively Q-switched laser waveform has also been illustrated as the comparison in Figure 3(b). It is obvious that the waveform of the actively Q-switched laser is disorder with the pulse width of 9.3 ns and the line width cannot be narrow because the cavity started oscillation with multiple longitudinal modes. Using the passively Q-switched technique, the clean Gaussian waveform and the narrow line width can be achieved because of the single longitudinal selection.

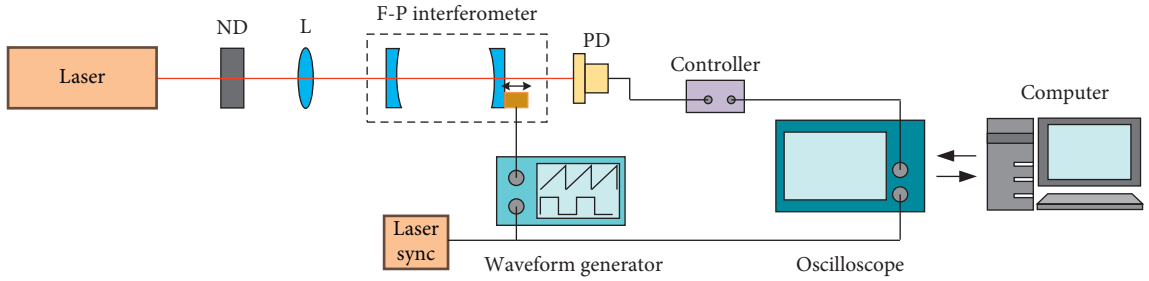

Figure 2: Schematics for scanning F-P interferometer method used in laser linewidth measurement.

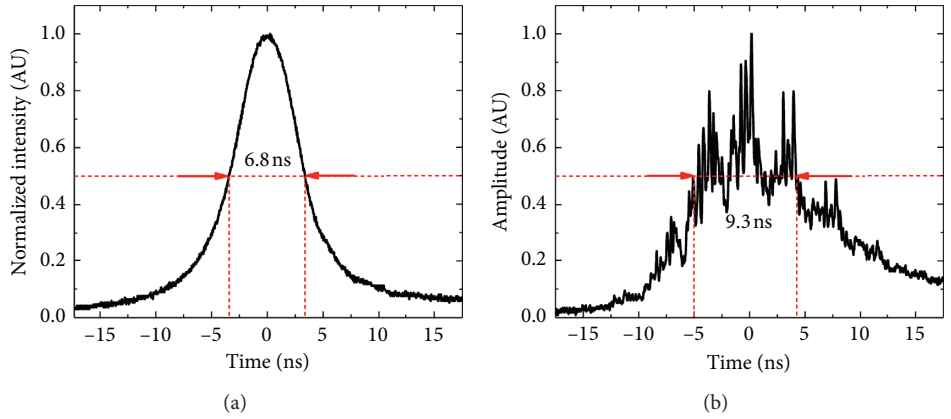

Figure 3: The temporal waveform of the output laser of the fundamental frequency: (a) the passively Q-switched laser output; (b) the actively Q-switched laser output.

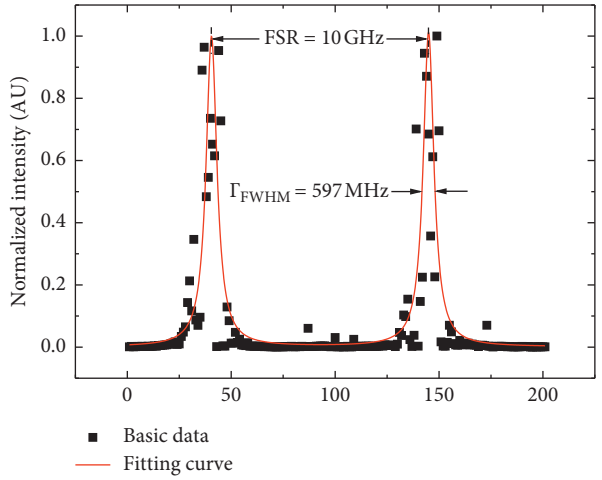

Figure 4: The spectrum of the passively Q-switched laser measured by the scanning F-P interferometer technique. FSR is the free spectral range of the etalon and Γ_{FWHM} is the laser line width.

Figure 4 illustrates the spectrum of the passively Q-switched laser. Each data point is the normalized amplitude integration of the F-P interferometer transmitted laser waveform under different driving voltage given by the waveform generator. The voltage rises evenly from 0 V to 7.5 V in the period of 100 seconds corresponding to the single FSR and sharply drops from 7.5 V to 0 V like a cliff where the reset time can be ignored. The discrete spectrum is fitted by the Lorentz function, and the line width of the passively Q-switch laser is measured to be 597 MHz. The line width is a little bit larger than the theoretical value since the thermal effect in the high power amplifier enhances the collision broadening. The line width of the actively Q-switched laser is much larger than the FSR of this F-P interferometer, theoretically exceeding 30 GHz [20].

In order to satisfy the needs at different application occasions, the passively Q-switched laser performance under different repetition rates was tested, as the results shown in

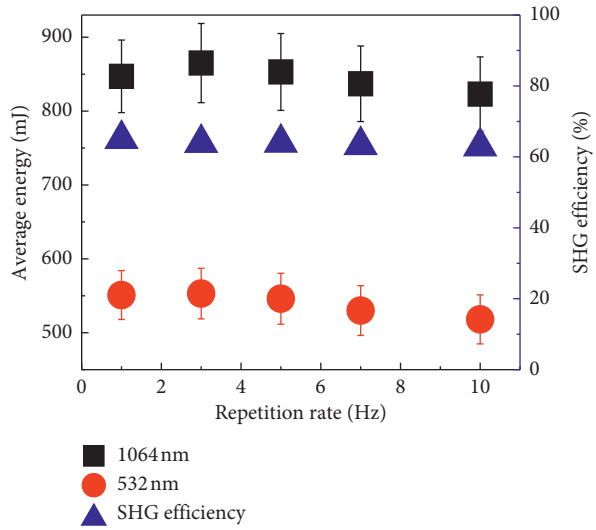

Figure 5: The average energy of 1064 nm and 532 nm laser and SHG Efficiency under different repetition rates.

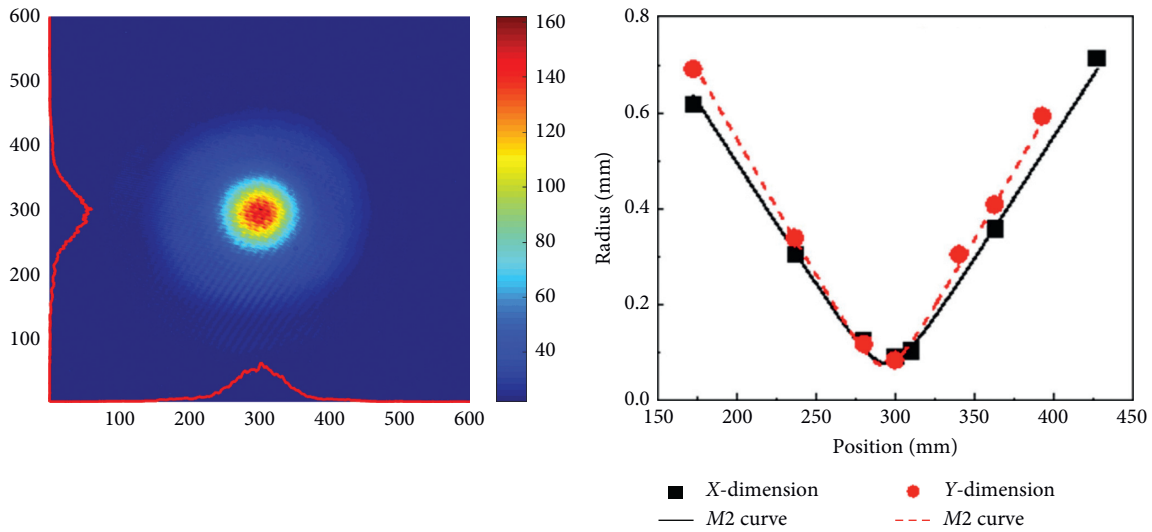

Figure 6: (a) The beam intensity profile of the SHG laser output measured by CCD and (b) the beam quality factors of M_x^2 and M_y^2 of the laser system.

Figure 5. Each point was calculated from 100 shots with other conditions same such as amplifiers voltage constant, and the energy of the fundamental frequency and the frequency doubling laser pulses were recorded simultaneously by inserting the wedge plates into the laser path and operating two energy meters. From the illustration, with the increase of the repetition rates, the pulses energy and the frequency conversion efficiency drop slightly. It is because of the waste heat accumulating during the operation in both laser crystal and the KTP. Overall speaking, the laser system maintains a stable operation under different rates, and the energy of 1064 nm and 532 nm reaches 860 mJ and 550 mJ separately. The RSD (relative standard deviation) of laser pulse energy is less than 6.2%.

The intensity distribution profiles after frequency doubling with pulse energy 500 mJ are shown in Figure 6(a). The measured beam diameter of near-field is about 6.3 mm in x-direction and 6.0 mm in y-direction. The profiles show that the SHG laser is operating at near TEM00 mode. On the condition of the maximum energy output, the beam radius measured from horizontal directions at different positions was recorded as shown in Figure 6(b). By means of the 90/10 knife edge method, we obtained the beam quality factors of $M_x^2 = 1.87$ and $M_y^2 = 2.34$ in x- and y-axes, respectively.

The output laser was diffracted by the rotating ground glass. The spot images were recorded by the scientific CCD, and the second-order correlation function was calculated by the computer. The CCD camera was positioned 1500 mm away from the G-glass. The pseudothermal light generated

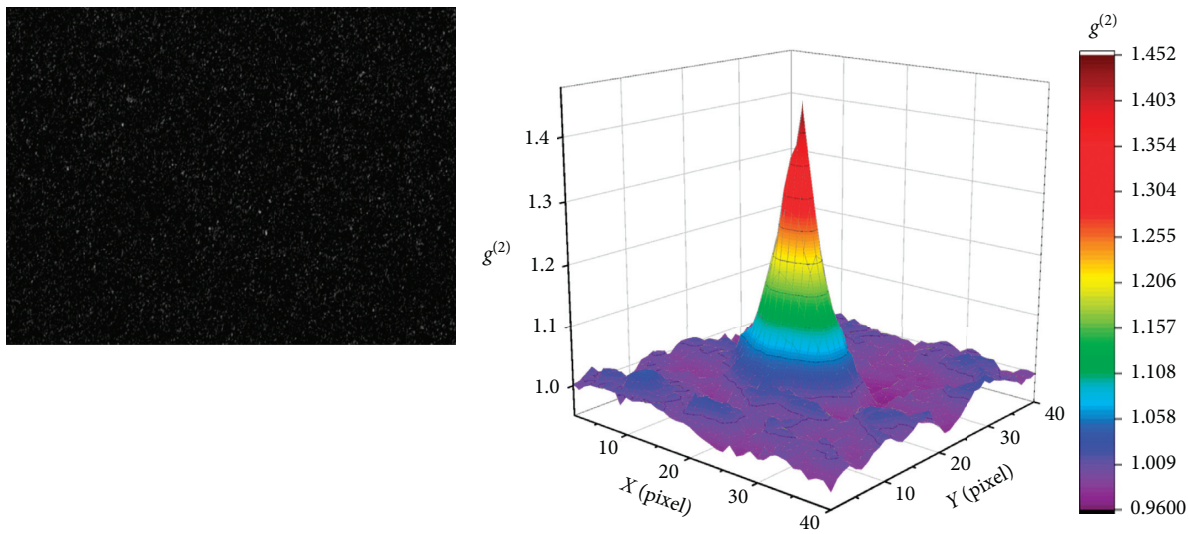

(a) (b)

FIGURE 7: The measured $g^{(2)}$ value of the actively Q-switched laser generating pseudothermal light: (a) the image achieved by CCD; (b) the corresponding pseudo-colour map of the second-order correlation function.

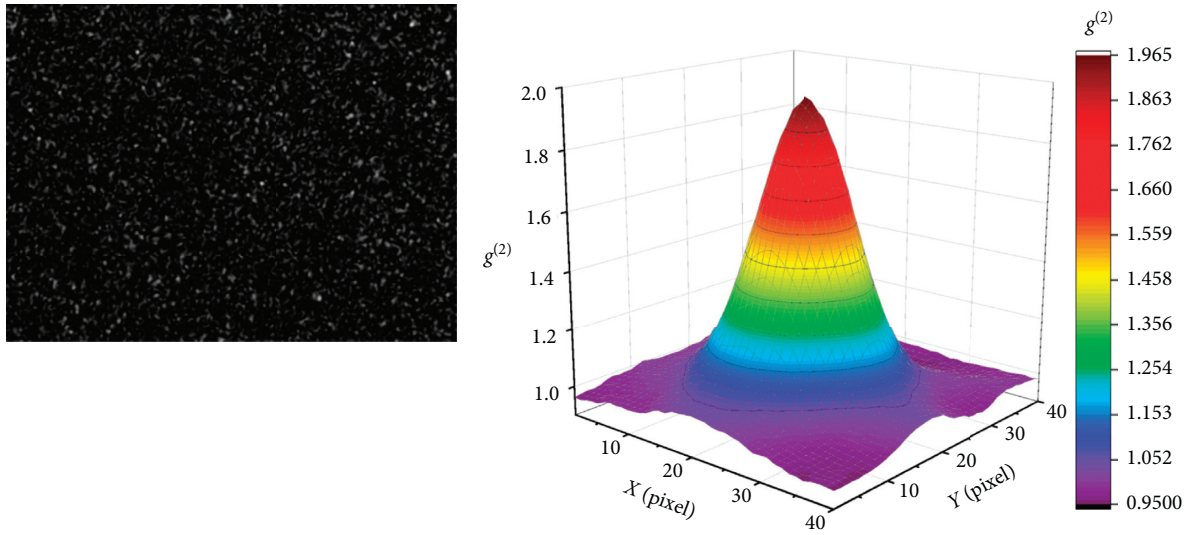

(a) (b)

FIGURE 8: The measured $g^{(2)}$ value of the passively Q-switched laser generating pseudothermal light: (a) the image achieved by CCD; (b) the corresponding pseudo-colour map of the second-order correlation function.

by the actively Q-switched laser was not in good quality. As Figure 7 illustrated, the second-order correlation function value of the pseudothermal light is 1.452. It is because the multilongitudinal mode operation shortens the coherence length of the light. The same experiment was carried out on the passively Q-switched laser system, and the second-order correlation function value of the pseudothermal light is 1.963 as illustrated in Figure 8, which is close the theoretical value of 2. The Cr^{4+}:YAG as a longitudinal selector suppresses the oscillator of the sideband frequency, resulting in the output laser with narrower bandwidth and longer coherence length. The pseudothermal light generated by the laser pulses with narrower bandwidth or single-longitudinal mode simulates the random intensity fluctuations of the classic thermal light field in a more realistic way, which makes it the ideal light source for the GI application.

4. Conclusions

In summary, a high power and high-visibility pseudothermal light has been demonstrated. Passively Q-switched method has been applied instead of active method to suppress the

sideband wavelength of oscillation to achieve extremely narrow bandwidth output. High damage threshold, large crystal size, and high energy-transferring efficiency of KTP guarantees the visible 532 nm laser output of over 500 mJ with 5 ns pulse width. With the second-order correlation function value close to 2 and stable output pulse energy, the pseudothermal light becomes an ideal and potential equipment for the airborne ghost imaging LiDAR. To achieve higher brightness pseudothermal light, the laser pulses with higher intensity will be required. Stimulated Brillouin scattering compression technology provides a great manner to compress the time duration to enhance the intensity of the laser pulses in the equivalent energy level; meanwhile, the intrinsic property of SBS material promises a great chance to gain the laser pulses with narrow bandwidth [21]. In future, the combination of SBS compression technology and the passively *Q*-switched laser will make the realization of the high-visibility high-brightness pseudothermal light possible.

Data Availability

The data used to support the findings of this study are included within the article. The data are original and have not been published before.

Conflicts of Interest

The authors declare that there are no conflicts of interest regarding the publication of this paper.

Acknowledgments

This study was supported by the project of the National Natural Science Foundation of China under Grant nos. 61927815 and 61905061 and the Hebei Science and Technology Innovation Strategy Funding Project (no. 20180601).

References

[1] W. Gong, C. Zhao, H. Yu, M. Chen, W. Xu, and S. Han, "Three-dimensional ghost imaging lidar via sparsity constraint," *Scientific Reports*, vol. 6, no. 1, Article ID 26133, 2016.

[2] Z. Kang, L. Ma, Y. Kang, Y. Yao, and T. Zhang, "Experiments of ghost imaging with pseudo-thermal light for remote sensing applications," *Applied Optics and Photonics China (AOPC2015) Optical and Optoelectronic Sensing and Imaging Technology*, vol. 9674, 2015.

[3] M. D'angelo, A. Valencia, M. H. Rubin, and Y. Shih, "Resolution of quantum and classical ghost imaging," *Physical Review A*, vol. 72, no. 1, Article ID 013810, 2005.

[4] C. Zhao, W. Gong, M. Chen et al., "Ghost imaging lidar via sparsity constraints," *Applied Physics Letters*, vol. 101, no. 14, Article ID 141123, 2012.

[5] R. E. Meyers, K. S. Deacon, and Y. Shih, "Turbulence-free ghost imaging," *Applied Physics Letters*, vol. 98, no. 11, Article ID 111115, 2011.

[6] J. Cheng, "Ghost imaging through turbulent atmosphere," *Optics Express*, vol. 17, no. 10, pp. 7916–7921, 2009.

[7] L. Zhang, Z. Lin, R. He, Y. Qian, Q. Chen, and W. Zhang, "Improving the noise immunity of 3D computational ghost imaging," *Optics Express*, vol. 27, no. 3, pp. 2344–2353, 2019.

[8] W. Gong and S. Han, "Experimental investigation of the quality of lensless super-resolution ghost imaging via sparsity constraints," *Physics Letters A*, vol. 376, no. 17, pp. 1519–1522, 2012.

[9] H. Liu, J. Cheng, and S. Han, "Cross spectral purity and its influence on ghost imaging experiments," *Optics Communications*, vol. 273, no. 1, pp. 50–53, 2007.

[10] C. Wang, X. Mei, L. Pan et al., "Airborne near infrared three-dimensional ghost imaging LiDAR via sparsity constraint," *Remote Sensing*, vol. 10, no. 5, p. 732, 2018.

[11] S. Han, H. Yu, X. Shen, H. Liu, W. Gong, and Z. Liu, "A review of ghost imaging via sparsity constraints," *Applied Sciences*, vol. 8, no. 8, p. 1379, 2018.

[12] P. Qiu, Z. Ye, Z. Bai, X. Liu, and S. Bo, "Computational ghost imaging with multiplexed time-varying signals," *International Journal of Optics*, vol. 2020, p. 8, Article ID 4109612, 2020.

[13] X. Liu, S. Bo, Z. Ye, P. Qiu, and J. Ding, "A Strategy for improving the quality of ghost imaging," *International Journal of Optics*, vol. 2020, no. 9703475, p. 8, 2020.

[14] Z. Bai, Y. Wang, Z. Lu et al., "A single -Longitudinal-Mode Nd:Ce:YAG Q-switched laser based on a three-plan resonant reflector," *Journal of Russian Laser Research*, vol. 37, no. 4, pp. 382–388, 2016.

[15] D. Jin, Z. Bai, Q. wang et al., "Doubly Q-switched single longitudinal mode Nd:YAG laser with electro-optical modulator and $Cr4^{+}$:YAG," *Optics Communications*, vol. 463, no. 8, Article ID 12500, 2020.

[16] J. H. Shapiro, D. Venkatraman, and F. N. C. Wong, "Ghost imaging without discord," *Scientific Reports*, vol. 3, no. 1, Article ID 1849, 2013.

[17] Y. Shih, Edited by L. Cohen, H. V. Poor, and M. O. Scully, Eds., "The Physics of Ghost Imaging," in *Classical, Semi-classical and Quantum Noise*, L. Cohen, H. V. Poor, and M. O. Scully, Eds., pp. 169–222, Springer, Berlin, Germany, 2012.

[18] J. H. Shapiro and R. W. Boyd, "The physics of ghost imaging," *Quantum Information Processing*, vol. 11, no. 4, pp. 949–993, 2012.

[19] X. Shen, M. Zhang, H. Liu, and S. Han, "Research on the pulsed pseudo-thermal light," *Chinese Journal Of Lasers*, vol. 36, no. 11, pp. 2893–2898, 2009.

[20] X. Wang and Z. Xu, "Single-longitudinal-mode operation of a 1 W combined actively and passively Q-switched Cr, Nd:YAG laser," *Optics Express*, vol. 13, no. 18, Article ID 6693, 2005.

[21] E. Garmire, "Stimulated brillouin review: invented 50 Years ago and applied today," *International Journal of Optics*, vol. 2018, p. 17, Article ID 2459501, 2018.